8. A. G. Goloveiko and V. I. Martynikhina, "Excitation of a temperature wave in a metal under the action of a square surface heat pulse," Inzh.-Fiz. Zh., 40, No. 3, 489-494 (1981).

FLOW OF A THIN FILM OF A VISCOUS LIQUID IN A GAS JET

Yu. I. Abramov

UDC 532.529.5

An approximate formulation is considered for the steady-state wave flow of a thin film of viscous liquid subject to tangential frictional stresses at the boundary. Measurements have been made on the stability limit for droplet detachment, and it has been found that the detachment rate and fractional composition of the droplets are dependent on the boundary conditions.

Vapor—liquid and gas—liquid media are widely used in power systems and various engineering devices, which has led to interest in flows of thin films of liquid at $Re_{fi} = 5$-400, which are characteristic of the natural conditions at the walls of equipment and the corresponding flow region with capillary waves on the surface [1].

There are papers [1, 2] on the basic laws of the wave motion of a thin film for flow in a constant field of mass forces, and these have been extended [3, 4]. However, the scheme used there did not have tangential frictional stresses at the free boundary of the film, so it was impossible to extend the conclusions and equations to the flow of a film in a gas jet, where the viscous interaction between the phases is responsible for tangential frictional stresses τ_0 at the interface.

We consider the case where the film is acted on by a mass force strength j, while the surface is in a gas flow, with the gas pressure constant along the flow direction ($\partial P''/\partial x = 0$); we assume that there is no heat or mass transfer in the wall—film—gas system, while τ_0 is taken as uniformly distributed over the film.

Following [1], the current thickness of the film is specified as

$$\delta = \delta_0 (1 + \varphi), \tag{1}$$

where φ is some function of the coordinate x and time t, which defines the deviation of the film thickness from the mean value δ_0.

We restrict consideration to steady-state wave flow, where any function of φ satisfies

$$\frac{\partial F(\varphi)}{\partial t} = -k \frac{\partial F(\varphi)}{\partial x}, \tag{2}$$

where k is the phase velocity of the waves.

We also assume that δ/λ and a/λ should be small.

With these assumptions, the wave flow can be described by a system of equations consisting of the equation of motion in the Navier—Stokes form:

$$\frac{\partial v_x'}{\partial t} + v_x' \frac{\partial v_x'}{\partial x} + v_y' \frac{\partial v_x'}{\partial y} = -\frac{1}{\rho'} \frac{\partial P'}{\partial x} + j_x + \frac{\mu'}{\rho'} \nabla^2 v_x' \tag{3}$$

and the equation of continuity

$$\frac{\partial (\rho' \bar{v}')}{\partial x} = -\frac{\partial \delta}{\partial t}, \tag{4}$$

where

Translated from Inzhenerno-Fizicheskii Zhurnal, Vol. 40, No. 4, pp. 622-630, April, 1981. Original article submitted February 4, 1980.

 0022-0841/81/4004-0368$07.50

$$\bar{v}' = \int_0^\delta v'_x dy.$$

It follows from (2) and (4) that

$$(k - \bar{v}')\,\delta = C, \tag{5}$$

where C is some constant determined by the flow rate in the film and the boundary conditions.

One expects that the mass forces and pressure gradient will produce a quadratic velocity distribution in the layer for a thin film, while the tangential frictional stresses at the free boundary will produce an additional velocity pattern, which will be close to linear. Therefore, the distribution of the longitudinal velocity in a layer with a film flowing under the combined forces can be put as

$$v'_x = \frac{3}{2}\left(\bar{v}' - \frac{1}{2}\,\frac{\tau_0}{\mu'}\,\delta\right)\left(\frac{2y}{\delta} - \frac{y^2}{\delta^2}\right) + \frac{\tau_0}{\mu'}\,y. \tag{6}$$

We assume that the velocity component v'_y is proportional to the distance from the wall, i.e.,

$$v'_y = v'_{y\delta}\frac{y}{\delta}\,.$$

The normal component of the velocity at the boundary is

$$v'_{y\delta} = \frac{d\delta}{dt} = \frac{\partial\delta}{\partial t} + v'_{x\delta}\,\frac{\partial\delta}{\partial x}\,,$$

so from (2) and (6) we get the distribution for the normal component of the velocity as

$$v'_y = \left(\frac{3}{2}\,\bar{v}' - k + \frac{1}{4}\,\frac{\tau_0}{\mu'}\,\delta\right)\frac{y}{\delta}\,\frac{\partial\delta}{\partial x}\,. \tag{7}$$

In (6) we have omitted small terms that incorporate the effects on v'_x from the derivative $\partial\delta/\partial x$, and therefore the requirement of equality for the tangential stresses at the phase interface with the velocity distribution in the film given by (6) and (7) is obeyed only approximately.

In a gradient-free gas flow, the pressure gradient in the liquid layer is set up by surface-tension forces arising from the curvature of the surface, and we can put approximately

$$\frac{\partial P'}{\partial x} = -\sigma\,\frac{\partial^3\delta}{\partial x^3}\,.$$

We integrate (3) over the thickness of the film for the velocity distribution given by (6) and (7) and use (2), (4), and (5) to convert to quantities averaged over the film thickness to get

$$\frac{\sigma}{\rho'}\,\delta^3\,\frac{\partial^3\delta}{\partial x^3} + k\,\frac{\mu'}{\rho'}\,\delta^2\,\frac{\partial^2\delta}{\partial x^2} + \Bigg[kC\delta + \frac{3}{20}\,(k^2\delta^2 - C^2) +$$

$$+\left(\frac{21}{40}\,C - \frac{3}{10}\,k\delta - \frac{3}{40}\,\frac{\tau_0}{\mu'}\,\delta^2\right)\frac{\tau_0}{\mu'}\sigma^2\Bigg]\,\frac{\partial\delta}{\partial x} + j_x\delta^3 + \frac{3}{2}\,\frac{\tau_0}{\rho'}\,\delta^2 + 3\,\frac{\mu'}{\rho'}\,(C - k\delta) = 0. \tag{8}$$

The wave function φ of (1) is introduced into (8), with restriction to terms of higher order, to get the following equation for the wave surface of the film in a first approximation:

$$\frac{\sigma}{\rho'}\,\delta_0^4\,\frac{\partial^3\varphi}{\partial x^3} + \Bigg[kC\delta_0 + \frac{3}{20}\,(k^2\delta_0^2 - C^2) + \Bigg(\frac{21}{40}\,C - \frac{3}{10}\,k\delta_0 -$$

$$-\frac{3}{40}\,\frac{\tau_0}{\mu'}\,\delta_0^2\Bigg)\,\frac{\tau_0}{\mu'}\,\delta_0^2\Bigg]\,\delta_0\,\frac{\partial\varphi}{\partial x} + 3\left(j_x\delta_0^3 + \frac{\tau_0}{\rho'}\,\delta_0^2 - \frac{\mu'}{\rho'}\,k\delta_0\right)\varphi + j_x\delta_0^3 + \frac{3}{2}\,\frac{\tau_0}{\rho'}\,\delta_0^2 + 3\,\frac{\mu'}{\rho'}(C - k\delta_0) = 0. \tag{8a}$$

The existence of a periodic solution to (8a) requires that the constant term should be zero, as should the coefficient φ. These conditions give us equations for the constants k and C:

$$k = \frac{\rho'}{\mu'}\left(\frac{\tau_0}{\rho'} + j_x\delta_0\right)\delta_0,\quad C = \frac{\rho'}{\mu'}\left(\frac{1}{2}\frac{\tau_0}{\rho'} + \frac{2}{3}j_x\delta_0\right)\delta_0^2. \tag{9}$$

For a given value of the flow rate q_V and motion in the field of mass forces, the mean thickness of a film with a wave surface is seen from (9) to be 20% less than the thickness of a film with an unperturbed surface. The thicknesses of the perturbed and unperturbed films agree to a first approximation when the motion is produced by the frictional force of the gas flow.

The stable periodic solution to (8a) is

$$\varphi = \alpha \sin nx, \tag{10}$$

where $\alpha = a/\delta_0$ and n satisfies

$$n^2 = \left[\frac{1}{2}\left(\frac{\tau_0}{\mu'}\right)^2 + \frac{17}{12}\frac{\rho'}{\mu'}\frac{\tau_0}{\mu'}j_x\delta_0 + \frac{3}{4}\left(\frac{\rho'}{\mu'}\right)^2 j_x^2\delta_0^2\right]\frac{\delta_0\rho'}{\sigma}. \tag{11}$$

Expression (11) can be transformed with respect to the flow rate q_V. For the case $\tau_0 = 0$ it takes the form

$$n^2 = \frac{9}{8}\frac{\rho'^2 j_x}{\mu'\sigma}q_v,$$

and for the case $j_x = 0$ it is

$$n^2 = \frac{\sqrt{2}}{2}\frac{\sigma}{\rho'}\left(\frac{\tau_0}{\mu'}\right)^{1.5} q_v^{0.5}.$$

The value of α can be found from the condition for energy stability of the wave flow [1]. For $j_x = 0$, e.g., the value of α is about 0.11.

We compare these approximate results with measurements for values of M for the gas flow in the range 0.10-0.95.

The working part of the system was a horizontal channel of rectangular cross section containing a smooth plate supplied with liquid at the start via a slot of width 0.2 mm, which produced a thin water film. Aerodynamic knife edges of height 4 mm at the sides of the plate eliminated leakage over the sides, while absorbing slots made it possible to monitor the flow along the plate.

Photography revealed the break-up of the wave pattern into individual parts, within each of which there was independent wave flow. The capillary waves had elevated steepness at the leading edge, which was due to higher harmonics [1], which were not incorporated in deriving (8a). The lengths of the capillary waves varied in each part and from one part to another, but on the whole the spread in λ was random. The median wavelength was particularly prominent in stroboscopic visualization and agreed with the value found from $\lambda = 2\pi/n$.

Figure 1 compares the observed and calculated wavelengths. Here τ_0 was estimated from the classical equations for a single-phase boundary layer [5], while the wave surface was identified with a rough one. The roughness was taken as twice the amplitude of the capillary waves. The data of [2] were also in agreement with the calculation.

On the whole, the good agreement over the wavelengths indicates that the equations from the approximate analysis are applicable to the linear characteristics under actual flow conditions.

The small capillary waves were accompanied by large single waves with elevated phase velocities, which have been described elsewhere [2, 6].

At high gas speeds, the mechanical interaction was accompanied by detachment and transport of droplets of liquid. The picture of the droplet transport was analogous to that described in [7].

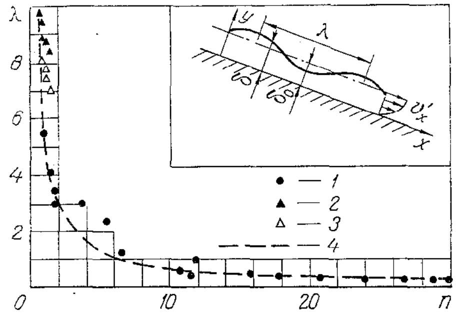

Fig. 1. Dependence of wavelength on flow rate q_V and boundary conditions: 1) water film in a gas jet; 2, 3) water and alcohol films, respectively, flowing under gravity [2]; 4) calculation. λ in mm and n in 1/mm.

The detached droplets moved in the comparatively narrow gas-droplet layer above the surface of the film, whose thickness increased in the flow direction. The mechanism of aerodynamic interaction between the droplets and the gas in this layer eliminated any repeated contact with the surface of the film. For example, if the film was drawn off through a slot, no film was seen to form in the subsequent parts of the plate, even for high droplet concentrations in the gas-droplet layer.

These results indicate that the transport of water from the surface of the film is to be ascribed to turbulence in the gas layer above the film rather than to the hydrodynamics of the wave flow. The turbulent structure in the gas layer is also responsible to some extent for the initial deformation of the wave surface, whose further development is provided by molecular friction in the gas flowing over the deformed liquid. Therefore, any system of dimensionless quantities that defines the stability limit for droplet transport must reflect explicitly or inexplicitly the state and mode of flow in the gas boundary layer. In that approach, one automatically incorporates the initial flow conditions, which have been shown [6] to have a marked effect.

We neglect the mass forces and follow the general rules of the theory of similarity and dimensions [8] to get the following system of primary dimensionless characteristics for the droplet transport stability:

$$\frac{\rho'' v'' l}{\mu''},\ \frac{\rho' v' l}{\mu'},\ \frac{\rho'' v''^2 l}{\sigma},\ \frac{q_{v*}}{v'' l},\ \frac{\rho'' v''^2}{\rho' v'^2},\ \frac{v''}{v'},$$

which can be reduced to the following system when the characteristic linear dimension l is taken as the thickness δ_g of the gas boundary layer:

$$\bar{\delta} = \delta_g \left(\frac{\rho'' v''^2}{\mu' q_{v*}} \right)^{0.5},\ \mathrm{Re}_\delta = \frac{\rho'' v'' \delta_g}{\mu''},\ F = \frac{\mu'' v''}{\sigma},\ \mathrm{Re}_{fi},\ \frac{\rho'' v''^2}{\rho' v'^2},\ \frac{v''}{v'} \tag{12}$$

with the three definitive criteria $\bar{\delta}$, Re_δ, and F, whose values are determined from the speed of the gas at the core of the gas flow.

Figure 2 shows the stability limit as a function of the definitive criteria of (12). This is closely approximated by

$$\bar{\delta} = 7.3 \cdot 10^2\ \mathrm{Re}_\delta^{0.76} F^{1.97}. \tag{13}$$

Equation (13) gives an inexplicity relationship between the wave amplitude and the linear characteristics of the gas boundary layer for a state of the film critical as regards droplet transport.

In the self-modeling region for the coefficient of friction at the boundary, the stability limit can be described by the simpler equation

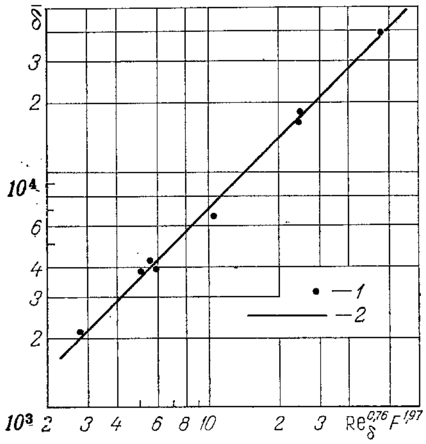

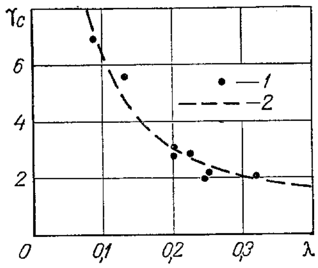

Fig. 2 Fig. 3

Fig. 2. Stability limit for droplet production as a function of the definitive criteria: 1) experiment; 2) calculation from (13).

Fig. 3. Dependence of the stabilized loss coefficient γ_c(1/m) on the wavelength at the surface of the film: 1) experiment; 2) calculation from (14).

$$q_{v*} = 63.5g\,\frac{\mu'\sigma}{\tau_0^2}\,.$$

Loss of liquid from the film is a consequence of the wave motion. The traveling wave acts as a piston that displaces liquid into parts of the gas boundary layer remote from the wall, where the perturbations and the gas velocity are sufficient to overcome the surface-tension forces, with the formation and detachment of droplets.

If we introduce the transport coefficient γ, which is defined as

$$\gamma = \frac{1}{q_v}\,\frac{\partial q_v}{\partial x}$$

and which characterizes the specific intensity of the transfer, then the mass transfer of liquid over a length l per unit width of flow is

$$M = \rho' \int_0^l \gamma(x)\, q_v dx.$$

The sources of the droplets are the ridges in the capillary waves, so it can be shown that the transfer rate should be proportional to the number of sources u, whose number is inversely proportional to the wavelength, i.e., $u \propto 1/\lambda$, as well as to the frequency of the wave oscillations on the surface $f = k/\lambda$ and the amount of liquid displaced by the traveling wave into the gas boundary layer during one period of oscillation over a length λ, i.e., $a\rho'\delta_0\lambda$.

With this relationship between the transport intensity and the film parameters, the coefficient should satisfy

$$\gamma = b/\lambda, \tag{14}$$

where b is a coefficient of proportionality dependent on the state and parameters of the gas boundary layer.

The experiment confirms (14), but only for flow rates in excess of some value q_{vc}, which exceeds q_{v*} by a factor 1.5-2.5 for the same conditions at the boundaries. In the range $q_{v*} < q_v < q_{vc}$, γ decreases monotonically from $\gamma = \gamma_c$ at $q_v \geq q_{vc}$ to $\gamma = 0$ at $q_v = q_{v*}$.

Figure 3 shows experimental data on the transport and calculation of (14). The value of b for an air-water mixture is $6.4 \cdot 10^{-4}$.

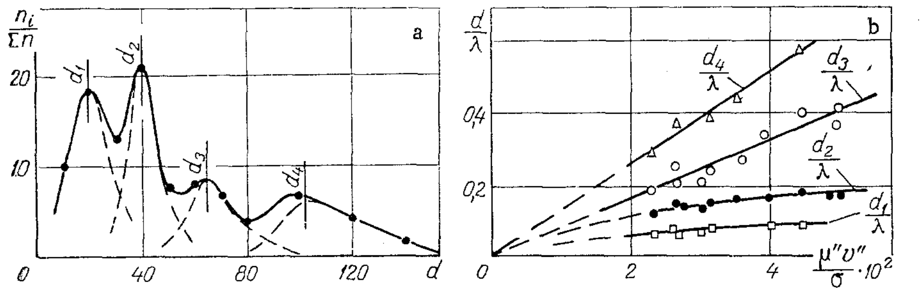

Fig. 4. Spectral characteristics of the flows of droplets: a) histogram for the droplet size distribution for v" = 110 m/sec; b) dependence of median dimensions of droplets on capillary wavelength and conditions at the free boundary; $n_i/\Sigma n$, %, d in μm.

Practical interest is attached to the fractional composition of the droplets, as well as to methods of quantitative evaluation.

Figure 4a gives a histogram for the size distribution, where the method of determination was described in [9] (n_i is the number of droplets of size $d_i \pm \Delta d_i$, where Σn is the number of droplets in the sample). For flow rates $q_v > q_{vc}$, the form of the histogram is typical for the entire range of subsonic gas speeds.

The results on the fractional composition and on the wave modes show that the group of droplets of large size, whose representative diameter is the median diameter d_4, corresponds to loss from the ridges of the large single waves. The frequency of occurrence of these is much less than the frequency of surface oscillation on the fundamental, but the large amplitude means that there is considerable loss from the ridges of these waves.

The group of droplets with median diameter d_3 corresponds to loss from the ridges of the capillary waves at the fundamental. The groups with median diameters d_1 and d_2 represent secondary droplets formed correspondingly in loss from the large and small waves.

The distribution over the sources is dependent on q_v. In the region $q_v > q_{vc}$, the predominant loss is from the ridges of the small capillary waves, which supply about 80% of the droplet liquid. In the region $q_{v*} < q_v < q_{vc}$, the reduced amplitude of the wave surface means that there is an increased fractional representation of the droplets from the large single waves, which become the only source for $q_v \approx q_{v*}$.

This shift in the distribution between sources is the main reason why (14) is not obeyed in the region $q_{v*} < q_v < q_{vc}$.

The loss of droplets is due to the wave mode of flow, and one therefore takes the unit for the linear scale of the droplet formation as the wavelength λ, while the median size may be related to the conditions at the boundary as some relationship between d/λ and a dimensionless quantity characterizing the relationship between the force fields acting on the film.

As the wave amplitude is small even by comparison with the thickness of the viscous sublayer, the resistance law for the deformed ridges can be taken as linear in the gas speed, and then the desired relationship is

$$\frac{d}{\lambda} = \beta \left(\frac{\mu'' v''}{\sigma} \right)^m, \tag{15}$$

where β and m are experimental coefficients.

TABLE 1. Coefficients in (15) in Terms of Median Droplet Sizes

Coefficients	Median droplet sizes			
	d_1	d_2	d_3	d_4
m	0,5	0,5	1	1
β	0,36	0,84	8,2	12,8

The experimental data were processed in this way as in Fig. 4b, while the values of β and m given by the median droplet sizes are given in Table 1. Figure 4 b shows that the size of the large droplets formed from the ridges of the capillary waves approximates to $\lambda/2$ at high speeds. A similar conclusion has been drawn from the data of [7], where it was shown that the entire ridge of a capillary wave is involved in droplet formation at high speeds.

NOTATION

Re_{fi}, Reynolds number for film; ρ, density; v, velocity; P, pressure; μ, viscosity; M, Mach number; q_V, volume flow rate per unit width; σ, surface tension; a, wave amplitude; λ, wavelength; τ_0, shear stress at free boundary; g, acceleration due to gravity, 9.81 m/sec^2; y, coordinate normal to wall. Indices: ', liquid phase; ", gas phase; δ, free film boundary; *, critical state of the film with respect to drop entrainment.

LITERATURE CITED

1. P. L. Kapitsa, "Wave flow in thin layers of viscous liquid," Zh. Eksp. Teor. Fiz., 18, No. 1, 3-18 (1948).
2. P. L. Kapitsa and S. P. Kapitsa, "Wave flow in thin layers of viscous liquid. An experimental study of the wave conditions of flow," Zh. Eksp. Teor. Fiz., 19, No. 2, 106-120 (1949).
3. V. Ya. Shkadov, "Wave modes of flow of a thin layer of viscous liquid under gravitational forces," Izv. Akad. Nauk SSSR, Mekh. Zhidk. Gaza, No. 1, 52-56 (1967).
4. V. Ya. Shkadov, "Theory of the wave flow of a thin layer of viscous liquid," Izv. Akad. Nauk SSSR, Mekh. Zhidk. Gaza, No. 2, 47-53 (1968).
5. G. N. Abramovich, Applied Gas Dynamics [in Russian], Nauka, Moscow (1969).
6. R. M. Yablonik and V. A. Khaimov, "Stability of film flow in short channels," Inzh.-Fiz. Zh., 25, No. 4, 641-646 (1973).
7. V. N. Bykov and M. E. Lavrent'ev, "Generation of the droplet-size spectrum in a gas-liquid flow," Inzh.-Fiz. Zh., 31, No. 5, 113-117 (1976).
8. L. I. Sedov, Methods of Similarity and Dimensions in Mechanics [in Russian], Nauka, Moscow (1967).
9. Yu. I. Abramov and A. V. Silin, "Formation of large water droplets at the outlet edges of nozzles in wet-steam turbines," Teploenergetika, No. 2, 31-34 (1977).